Tree Physiology 37, 851–868
doi:10.1093/treephys/tpx011

Research paper

A steady-state stomatal model of balanced leaf gas exchange, hydraulics and maximal source–sink flux

Teemu Hölttä[1], Anna Lintunen, Tommy Chan, Annikki Mäkelä and Eero Nikinmaa

Department of Forest Sciences, University of Helsinki, Latokartanonkaari 7, PO Box 27, 00014 Helsinki, Finland; [1]Corresponding author (teemu.holtta@helsinki.fi)

Received July 30, 2016; accepted January 23, 2017; published online February 23, 2017; handling Editor Maurizio Mencuccini

Trees must simultaneously balance their CO_2 uptake rate via stomata, photosynthesis, the transport rate of sugars and rate of sugar utilization in sinks while maintaining a favourable water and carbon balance. We demonstrate using a numerical model that it is possible to understand stomatal functioning from the viewpoint of maximizing the simultaneous photosynthetic production, phloem transport and sink sugar utilization rate under the limitation that the transpiration-driven hydrostatic pressure gradient sets for those processes. A key feature in our model is that non-stomatal limitations to photosynthesis increase with decreasing leaf water potential and/or increasing leaf sugar concentration and are thus coupled to stomatal conductance. Maximizing the photosynthetic production rate using a numerical steady-state model leads to stomatal behaviour that is able to reproduce the well-known trends of stomatal behaviour in response to, e.g., light, vapour concentration difference, ambient CO_2 concentration, soil water status, sink strength and xylem and phloem hydraulic conductance. We show that our results for stomatal behaviour are very similar to the solutions given by the earlier models of stomatal conductance derived solely from gas exchange considerations. Our modelling results also demonstrate how the 'marginal cost of water' in the unified stomatal conductance model and the optimal stomatal model could be related to plant structural and physiological traits, most importantly, the soil-to-leaf hydraulic conductance and soil moisture.

Keywords: phloem transport, photosynthesis, process based model, stomatal control, xylem transport.

Introduction

Water and carbon exchange occur in opposing directions in a tightly controlled manner at the vegetation–atmosphere interface through stomatal openings in the leaves of vascular plants. The loss of water from the leaves to the atmosphere is replaced with water flow from soil through the xylem, while part of the xylem sap flow is needed for turgor-driven transport of the assimilated carbohydrates in the phloem from leaves to sites of consumption in sugar sinks. Xylem transport and water uptake by roots have to maintain the rate of water loss by transpiration from the leaves, or stomatal closure will have to occur to prevent excessive decrease in xylem water potential and the associated plant dehydration and run-away embolism in the xylem (Tyree and Sperry 1988). Similarly, symplastic osmotic concentrations need to match the hydrostatic pressure drop in the leaves and phloem transport and utilization of photosynthates in sinks have to match the rate of carbon assimilation in photosynthesis, or carbohydrate accumulation will eventually force stomatal closure and down-regulation of photosynthesis (Paul and Foyer 2001).

While the exchange of water between leaves and atmosphere is determined mostly by stomatal conductance and water vapour concentration difference (VPD) between the intercellular spaces and ambient air, the situation for CO_2 exchange is more complex. The CO_2 concentration difference between the ambient air and intercellular spaces is dependent on the rate of CO_2 consumption inside the leaf mesophyll cells. There are complex feedbacks between the amount of light energy, leaf internal CO_2 concentration and the internal state of the leaf, e.g., its water and carbohydrate relations (Paul and Pellny 2003), which are further connected to the state of whole-tree water and carbon status

through xylem and phloem transport (Nikinmaa et al. 2013). While the trade-off between CO_2 assimilation and water vapour loss has been extensively treated in connection with plant water relations, the connection between transpiration-driven hydrostatic pressure and the photosynthesis-driven osmotic pressure has not, although the latter has implications for assimilate transport and their use in growth (DeSchepper and Steppe 2010, Hölttä et al. 2010). Due to the osmotic properties of the most common form of assimilated sugars, there is a relatively narrow margin between the feasible apoplastic water pressure and symplastic sugar concentration to maintain turgor pressure within physiologically reasonable limits, and indeed, disruptions in this balance have been suggested as one major cause of drought-related mortality (McDowell et al. 2011, Sevanto et al. 2014).

Stomatal responses to environmental and internal factors have been under rigorous study for the past decades, but the topic is still far from being understood. Our present understanding on stomatal behaviour is mainly based on relations of gas exchange at the leaf surfaces (Ball et al. 1987, Medlyn et al. 2011). Stomata appear to respond to VPD and light in a manner that optimizes water loss per carbon gain in a given leaf environment (Hari and Mäkelä 2003, Medlyn et al. 2011). In addition, factors not directly connected to leaf level relations such as soil water availability (Tuzet et al. 2003, Duursma et al. 2008), changes in xylem conductivity (Sperry et al. 1993), soil-to-leaf hydraulic conductivity (Rodriguez-Dominguez et al. 2016) and the utilization of photosynthates in sinks (Körner 2003) are known to play an important role in stomatal regulation. It is well acknowledged that many whole-plant level traits are involved in stomatal regulation, but a coherent framework that includes all of these is lacking. It has also become evident during recent years that besides the changes in stomatal conductance, also changes in mesophyll conductance and the biochemistry of photosynthesis contribute to the rate of photosynthetic production. The changes in mesophyll conductance are known to vary according to environmental conditions, even on time scales as short as minutes (Flexas et al. 2008, 2012, Kaiser et al. 2015), and the changes in mesophyll conductance and stomatal conductance appear to be tightly coupled (Gago et al. 2016). Also, the biochemistry of photosynthesis, i.e., carboxylation efficiency, has been found to change diurnally even during non-water stressed conditions (Guo et al. 2009, Buckley and Diaz-Espejo 2015). Although the details on how the stomatal and non-stomatal factors controlling photosynthesis are co-regulated are still missing, stomatal conductance and mesophyll conductance have typically been found to change in parallel (Flexas et al. 2008).

In this study, we develop a whole-tree-level theoretical framework to explain stomatal behaviour, and present a model linking carbon source (leaf gas exchange) and carbon sink (sugar utilization and soil water uptake) relations through xylem and phloem transport. The model is used to demonstrate how stomatal gas exchange is constrained by soil water status, sink strength, xylem and phloem transport, and the state of photosynthetic machinery as well as its sensitivity to local water and sugar status, in addition to the leaf level environmental conditions. The model employed is a steady-state simplification of the dynamic model used in Nikinmaa et al. (2013), where it was demonstrated that the stomatal behaviour of trees could be predicted by maximizing the instantaneous phloem mass transport rate. In relation to Nikinmaa et al. (2013), the steady-state formulation presented here is more straightforward, easier to implement and allows a closed form solution of the equations. We use the steady-state model to demonstrate that the stomatal behaviour of trees can be understood quite far in terms of maximizing the photosynthetic rate while being able to transport the assimilated sugars through the phloem and utilize the sugars in sinks in steady state (Hölttä and Nikinmaa 2013).

A key feature in our model is that it allows for the impact of source–sink linking to stomatal behaviour through the feedback between non-stomatal limitations to photosynthesis mediated by leaf water and/or carbohydrate status. We use the term non-stomatal limitations to photosynthesis to describe the decrease in photosynthesis rate for a given internal leaf CO_2 concentration, light level and temperature. The non-stomatal limitations arise due to metabolic impairment of photosynthesis and/or decrease in mesophyll conductance (Flexas and Medrano 2002). In our model framework the feedback between stomatal and non-stomatal limitations to photosynthesis arises as stomatal opening monotonically decreases leaf water potential and increases leaf sugar concentration (as shown in the Results section).

Our approach offers a coherent framework of stomatal regulation within whole-tree physiology. The predictions for stomatal control using our model approach span over a wider range of environmental, structural and physiological conditions in comparison with earlier stomatal control models, including the effects of drought and varying sink strength. Our model predictions for stomatal conductance are demonstrated to be very similar to the predictions given by the 'unified stomatal control model' (Medlyn et al. 2011) and the 'optimal stomatal conductance model' (Hari and Mäkelä 2003).

Materials and methods

Interactions between source, transport and sink

The interconnections and the underlying mathematical formulation used amongst transpiration, photosynthesis, xylem and phloem transport, soil water status and sink sugar status are depicted in Figure 1. The driving forces of water vapour and CO_2 exchange with the atmosphere through the stomata are the difference in their concentrations between the ambient air and leaf internal space. The utilization of CO_2 in photosynthesis creates and maintains the difference in the CO_2 concentration required for CO_2 inflow. The sugars assimilated by photosynthesis are

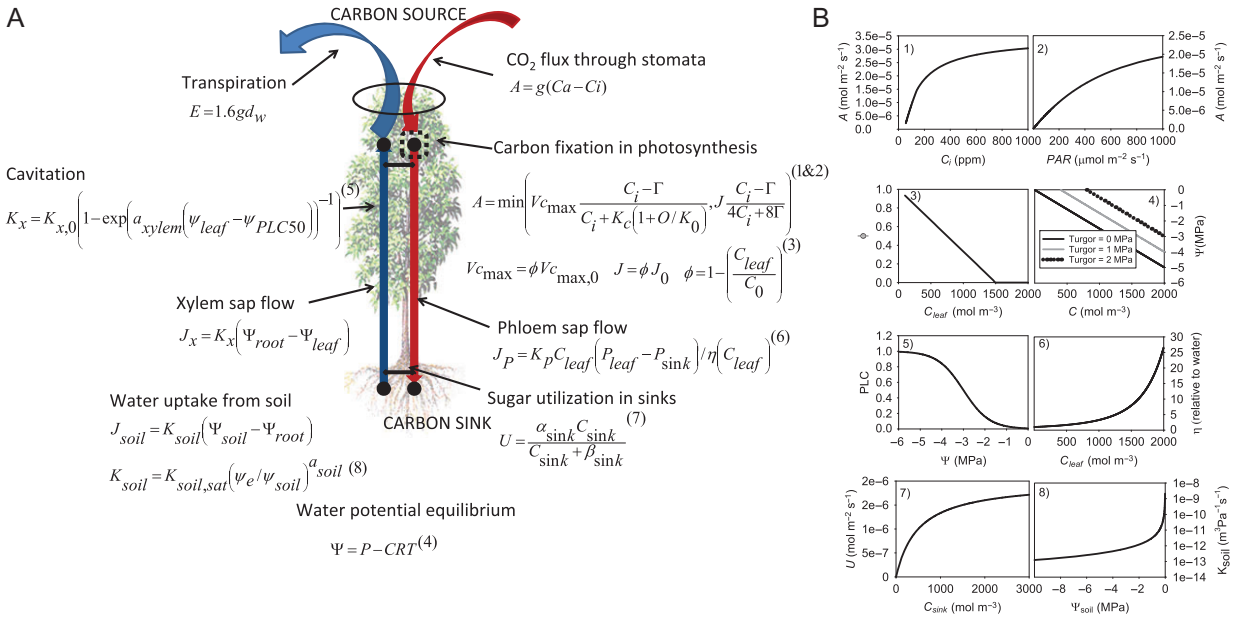

Figure 1. (A) Connections between source, transport and sink processes, and the governing equations used in the model expressed in mathematical relations. (B) The mathematical formulations demonstrated as graphs with the actual parameterizations used in the base case simulations.

passed passively along the concentration gradient in most tree species (Turgeon 2010) from the mesophyll cells to the phloem. The assimilated sugars draw water osmotically to the leaf phloem from the adjacent xylem tissue to maintain water potential equilibrium and simultaneously increase phloem hydrostatic (turgor) pressure. This positive pressure in the leaf phloem pushes water and dissolved sugars in the direction of the pressure gradient towards locations where the sugars are used in carbon sinks. Sugar utilization in the sink lowers the sink osmotic concentration, and also the turgor pressure as water potential equilibrium between the xylem and phloem is maintained at all locations in the tree. In the absence of sufficient sugar utilization in the sink, sugar concentration increases in the phloem and also in the leaves.

An important aspect is that all of the processes described in Figure 1 are coupled to each other and constrained by one another. A change in one variable, e.g., pressure, concentration, resistance or enzymatic rate constant (e.g., V_{cmax} in leaf or α_{sink} in sink), at one location will induce changes in pressure and concentration at all other locations within the plant. In steady state, the transpiration rate (E) must equal xylem sap flow rate (J_x) and rate of water uptake from the soil. CO_2 assimilation rate (A) must equal the phloem sap flow rate (J_p), which in turn must equal the rate of sugar utilization at sink. Xylem and phloem are tightly hydraulically coupled (Pfautsch et al. 2015, Steppe et al. 2015) so that phloem turgor pressure plus osmotic pressure must equal xylem water potential in all parts of the tree. Xylem conductance (k_x) is dependent on xylem water potential due to embolism formation by cavitation, and phloem conductance is dependent on sugar concentration due to viscosity. Transpiration, soil water availability, photosynthesis and sugar utilization at the sinks, and the conductances for diffusion and mass flow, set the gradients for xylem and phloem transport. Our numerical model consists of one source and one sink, which represent the leaves and roots, respectively (Figure 1A). The source and sink are connected by xylem and phloem transport.

Model description

Leaf gas exchange The driving force for stomatal gas exchange of CO_2 is the difference between the CO_2 concentration in ambient air (C_a, molar fraction of CO_2 in ambient air) and CO_2 concentration in the intercellular air spaces inside the leaves (C_i, molar fraction of CO_2 in the intercellular air spaces). The (leaf-area specific) rate of CO_2 diffusion (D_{CO_2}, mol $m^{-2}s^{-1}$) to the leaf internal space is as follows:

$$D_{CO_2} = g(C_a - C_i) \quad (1)$$

where g is the total diffusive conductance to CO_2 between leaf and air consisting of stomatal conductance (g_s, mol m^{-2} s^{-1}) and aerodynamic conductance (g_a, mol m^{-2} s^{-1}) ($g^{-1} = g_s{}^{-1} + g_a{}^{-1}$). Similarly for water, the rate of (leaf-area specific) water vapour diffusion to the air (E, m^3 m^{-2} s^{-1}) is as follows:

$$E = 1.6g(W_i - W_a)F_{mol\_m3} = 1.6gd_wF_{mol\_m3} \quad (2)$$

where W_i and W_a are the intercellular and ambient molar fractions of water vapour (mol_{H_2O}/mol_{air}), F_{mol_m3} is a factor (18×10^{-6} m^3 mol^{-1}) for converting the units of transpiration rate from mol m^{-2} s^{-1} to m^3 m^{-2} s^{-1} to match the units of xylem water transport rate (Eq. (8)) and d_w is vapour pressure deficit

(VPD, mol_{H_2O}/mol_{air}). The factor 1.6 in Eq. (2) arises as stomatal and aerodynamic conductances are expressed for CO_2, and the corresponding value for water is 1.6 times larger.

Leaf temperature was modelled to be a function of ambient air temperature, irradiation and leaf transpiration rate according to the following equation from Jones (1992):

$$T_{leaf} = T_{amb} + \frac{r_{HR}(r_{aW} + r_{IW})\gamma\Theta_{ni}}{\rho_a c_p[\gamma(r_{aW} + r_{IW}) + sr_{HR}]} - \frac{r_{HR}d_w}{\gamma(r_{aW} + r_{IW}) + sr_{HR}} \quad (3)$$

where T_{leaf} is leaf temperature, T_{amb} is ambient temperature, r_{HR} is heat transfer resistance from the leaf, r_{aW} is leaf boundary layer resistance to water vapour ($r_{aW} = r_{HR} = 1/(1.6 \times g_a)$), r_{IW} is stomatal resistance to water vapour ($r_{IW} = 1/(1.6 \times g_s)$), γ is the psychrometric constant, ρ_a is air density, c_p is the specific heat capacity of air, s is the slope of the curve relating saturation vapour pressure to temperature, and Θ_{ni} is net isothermal radiation. r_{aW} and r_{HR} are dependent on wind speed and leaf width. r_{aW} and r_{HR} were assumed to be the same, and they were given a value of 13 s m^{-1}, a typical value for thin leaves given in Nobel (2005). This corresponds to an approximately 2.4 °C increase in leaf temperature per 1000 μmol m^{-2} s^{-1} photosynthetically active radiation (PAR) for the base case simulation. This magnitude is in accordance with a value reported for Scots pine tree by Kolari et al. (2007), who reported a 1.5 °C increase in leaf temperature per 1000 μmol m^{-2} s^{-1} for a Scots pine tree. Net isothermal radiation was assumed to be equal to one-quarter of PAR (Barbour et al. 2000).

At steady state, the rate of CO_2 consumption in photosynthesis in the chloroplasts (A) must be the same as the rate of diffusion from the ambient air (D_{CO_2}). Photosynthesis was modelled according to the Farquhar model (Farquhar et al. 1980, Sharkey et al. 2007):

$$A = \min\left(V_{c\,max}\frac{C_i - \Gamma}{C_i + K_c(1 + O/K_O)},\ J\frac{C_i - \Gamma}{4C_i + 8\Gamma}\right) \quad (4a)$$

where

$$J = \frac{ql + J_{max} - \sqrt{(ql + J_{max})^2 - 4\Theta ql J_{max}}}{2\Theta} \quad (4b)$$

and V_{cmax}, J, J_{max}, Γ, K_c, O, K_o, q, Θ are the parameters of the Farquhar photosynthesis model (Table 1), and I is light intensity.

The photosynthetic parameters V_{cmax} and J were made to be dependent on leaf sugar concentration to account for the changes in the non-stomatal limitations to photosynthesis. The changes in the non-stomatal limitations to photosynthesis were modelled by multiplying the maximum values of V_{cmax} and J, $V_{cmax,O}$ and J_O (given in Table 1), respectively, by a unitless factor ϕ ($\phi \leq 1$).

$$V_{c\,max} = \phi V_{c\,max,O} \quad (5a)$$

and

$$J = \phi J_O \quad (5b)$$

Because the functional form for the relationship between the changes in the non-stomatal limitations to photosynthesis and leaf sugar concentration is not known, we applied a linear relationship between them

$$\phi = 1 - \frac{C_{leaf}}{C_O} \quad \text{if } C_{leaf} < C_o (\phi = 0 \text{ if } C_{leaf} > C_o) \quad (6)$$

where C_{leaf} is leaf sugar concentration and C_O is the leaf sugar concentration at which photosynthesis vanishes. A similar function of linearly increasing non-stomatal limitations to photosynthesis with increasing leaf sugar concentration was used in the models of Nikinmaa et al. (2013) and Mencuccini et al. (2015) and is also supported by the measurements in this study (Figure 2). Changes in V_{cmax} and J were here conducted simultaneously (see Eqs (5) and (6)) as they typically vary in concert (Wullschleger 1993, Meir et al. 2002, Zhou et al. 2013). Leaf respiration was not included in the model formulation to simplify the presentation. Photosynthesis rate was modelled as a function of leaf internal CO_2 concentration (C_i), instead of CO_2 concentration in chloroplasts. This way the changes in V_{cmax} and J implicitly include the changes in both mesophyll conductance and in the biochemistry of photochemistry, i.e., changes in RuBP utilization and regeneration. We do not attempt to partition the non-stomatal limitations to these different components in this study.

In addition, the photosynthetic parameters V_{cmax} and J_{max} were made to be temperature dependent according to the following approximation (Thum et al. 2007):

$$f_T = f_{T,0}\exp\left(\frac{E_f(T - 290)}{290RT}\right) \quad (7)$$

where f_T is either V_{cmax} or J_{max}, $f_{T,O}$ is V_{cmax} or J_{max} at a reference temperature of 17 °C, and E_f is the activation energy.

Non-stomatal limitations to photosynthesis have been quantified as a function of both leaf sugar content (C_{leaf}), e.g., in Turnbull et al. (2002) and Franck et al. (2006) and leaf water potential (Kellomäki and Wang 1996, Zhou et al. 2014). Modelling the non-stomatal limitations as a function of leaf water potential would lead to a very similar outcome except in the situation where sink strength changes since leaf water potential and osmotic concentration are in other cases very well coupled. The formulation used, i.e., the sugar concentration dependence, allows us to capture the effects of both water stress and decreased sink sugar utilization rate on photosynthesis and stomatal conductance.

Since the relation between leaf sugar concentration and the non-stomatal limitations to photosynthesis turn out to be important relations affecting the model behaviour and so few quantitative

Table 1. List of symbols, environmental drivers and parameters (based on a typical day for Scots pine trees at SMEAR II station in Hyytiälä, Southern Finland, when possible).

Symbol	Meaning
E	Leaf-area specific transpiration rate ($m^3\ m^{-2}\ s^{-1}$)
J_x	Leaf-area specific xylem sap flow rate ($m^3\ m^{-2}\ s^{-1}$)
J_{soil}	Leaf-area specific rate of root water uptake from soil ($m^3\ m^{-2}\ s^{-1}$)
A	Leaf-area specific CO_2 assimilation rate ($mol\ m^{-2}\ s^{-1}$)
J_p	Leaf-area specific phloem sap flow rate ($mol\ m^{-2}\ s^{-1}$)
U	Leaf-area specific phloem unloading rate of sugars ($mol\ m^{-2}s^{-1}$)
Ψ_{leaf}	Leaf water potential (MPa)
Ψ_{root}	Root water potential (MPa)
Ψ_{soil}	Soil water potential (MPa)
C_{leaf}	Leaf phloem sugar concentration ($mol\ m^{-3}$)
C_{sink}	Sink phloem sugar concentration ($mol\ m^{-3}$)
P_{leaf}	Leaf phloem turgor pressure (MPa)
P_{sink}	Sink phloem turgor pressure (MPa)
g_s	Stomatal conductance for CO_2 ($mol\ m^{-2}\ s^{-1}$)[1]
g_a	Leaf aerodynamic conductance for CO_2 ($mol\ m^{-2}\ s^{-1}$)[1]
g	Total leaf to air conductance for CO_2 ($mol\ m^{-2}\ s^{-1}$)[1]
F_{mol_m3}	Unit conversion factor ($18 \times 10^{-6}\ m^3\ mol^{-1}$)
K_x	Xylem hydraulic conductance ($m\ Pa^{-1}\ s^{-1}$)
K_{soil}	Soil hydraulic conductance ($m\ Pa^{-1}\ s^{-1}$)
K_{tot}	Soil-to-leaf hydraulic conductance ($m\ Pa^{-1}\ s^{-1}$)[2]
ϕ	Relative decrease in A due to non-stomatal limitations (unitless)
C_i	Leaf internal CO_2 concentration (ppm)
R	A physical constant ($8.314\ J\ K^{-1}\ mol^{-1}$)
T	Temperature (300 K)[3]
η	Viscosity of phloem sap (unitless)[4]
Θ_{ni}	Net isothermal radiation ($W\ m^{-2}$)
Environmental driver	**Base case value**
C_a, Ambient CO_2 concentration	400 ppm
d_w, Vapour pressure deficit (VPD)	$0.01\ mol\ mol^{-1}$
I, Light intensity (PAR)	$200\ \mu mol\ m^{-2}\ s^{-1}$
Ψ_{soil}, Soil water potential	−0.1 MPa
T_{amb}, Ambient air temperature	17 °C
Parameter	**Base case value**
ψ_{PLC50}, ψ at which half of xylem conductance is lost	−3 MPa (Cochard 2006)
A_c, Slope of the xylem vulnerability curve	$2 \times 10^{-6} Pa^{-1}$ (Estimated)
$K_{x,O}$, Leaf-area specific xylem conductance	$4 \times 10^{-13}\ m\ Pa^{-1}s^{-1}$[5]
K_p, Leaf-area specific phloem conductance	$3 \times 10^{-14}\ m\ Pa^{-1}s^{-1}$[5]
$K_{soil,sat}$, Hydraulic conductance of saturated soil	$10 \times 10^{-6}\ m^3Pa^{-1}s^{-1}$ (based on Duursma et al. 2008)
Ψ_e, Soil parameter	−0.68 kPa (Duursma et al. 2008)
a_{soil}, Soil parameter	2.4 (based on Duursma et al. 2008)
α_{sink} and β_{sink}, Sink parameters	$5 \times 10^{-5}\ mol\ s^{-1}$ and $500\ mol\ m^{-3}$[6]
C_O, C_{leaf} at which photosynthesis goes to zero	$1500\ mol\ m^{-3}$[7]
$V_{cmax,O}$, Farquhar photosynthesis model parameter	$50 \times 10^{-6}\ mol\ m^{-2}\ s^{-1}$[8]
$J_{max,O}$, Farquhar photosynthesis model parameter	$110 \times 10^{-6}\ mol\ m^{-2}\ s^{-1}$[8]
Γ, Farquhar photosynthesis model parameter	38 ppm
O, Farquhar photosynthesis model parameter	210,000 ppm
K_o, Farquhar photosynthesis model parameter	420,000 ppm
K_c, Farquhar photosynthesis model parameter	275 ppm
θ, Farquhar photosynthesis model parameter	0.5
q, Farquhar photosynthesis model parameter	0.14
E_f, Activation energy	$65{,}000\ J\ mol^{-1}$[9]
γ, Psychrometric constant	$66.1\ MJ\ kg^{-1}$ (at ~20 °C)
c_p, Specific heat capacity of air	$1012\ J\ kg^{-1}\ K^{-1}$ (at ~20 °C)

(*Continued*)

Table 1. (Continued)

Parameter	Base case value
ρ_a, Air density	1.2 kg m^{-3} (at ~20 °C)
s, Slope of the curve relating saturation vapour pressure to temperature	145 Pa $°C^{-1}$ (at ~20 °C)
r_{HR}, Heat transfer resistance from the leaf	13 s m^{-1} (at ~20 °C)
r_{aW}, Leaf boundary layer resistance to water vapour	13 s m^{-1} (at ~20 °C)

[1]Expressed per total leaf area (and not projected leaf area) for CO_2. The conductance for water is 1.6 times higher.
[2]$K_{tot} = (K_x^{-1} + K_{soil}^{-1})^{-1}$.
[3]Used only in calculating osmotic potential.
[4]Expressed in relation to pure water (0.001 Pa s), for phloem viscosity is calculated as a function of phloem sugar concentration.
[5]Based on Nikinmaa et al. (2013).
[6]Chosen so that sink osmotic concentration would be reasonable, ~300 mol m^{-3}, which we have typically measured on Scots pine trees (unpublished).
[7]Laboratory measurements on seedlings showed ~1000 mol m^{-3} (Figure 2A), but this was increased to 1500 mol m^{-3} to match field observations.
[8]At a temperature of 17 °C. Based on Kolari et al. (2014) for Scots pine trees.
[9]Thum et al. (2007).

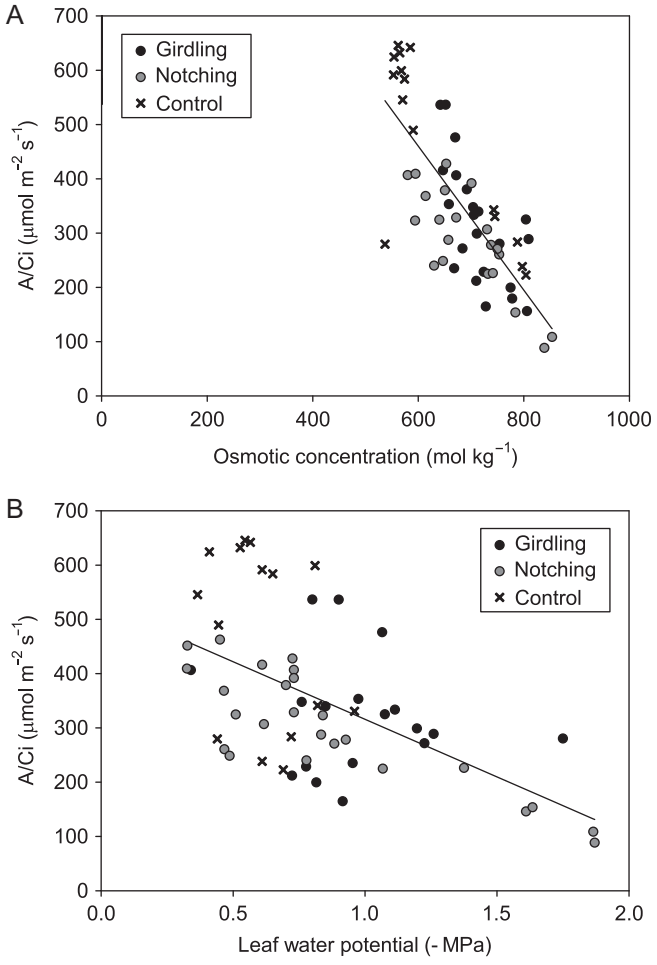

Figure 2. (A) Measured relations between leaf osmolality and the ratio between photosynthesis rate (A) and leaf internal CO_2 concentration C_i. (B) Measured relations between leaf water potential and the ratio between photosynthesis rate (A) and leaf internal CO_2 concentration C_i.

descriptions of this relation can be found in the literature, we performed laboratory measurements to approximately quantify this relation for Scots pine seedlings (see Laboratory measurements).

Xylem and phloem transport Leaf-area specific water flux from the root to the leaf (J_x) is described as a function of the leaf-area specific xylem hydraulic conductance (K_x, m Pa^{-1} s^{-1}), which decreases with decreasing water potential due to cavitation according to a Pammenter type vulnerability curve (Pammenter and Van der Willingen 1998), and the water potential difference between the root (ψ_{root}) and leaf (ψ_{leaf})

$$J_x = K_x(\psi_{root} - \psi_{leaf}) = K_{x,0}\left(1 - \exp\left(a_{xylem}(\psi_{leaf} - \psi_{PLC50})\right)^{-1}\right)(\psi_{root} - \psi_{leaf}) \quad (8)$$

where a_{xylem} is the slope of the vulnerability curve and ψ_{PLC50} is the water potential where half of the initial hydraulic conductance of the xylem $K_{x,0}$ has been lost due to cavitation. Note that here we do not take into account that the water potential varies along the xylem pathway, but the loss of hydraulic conductance in the whole tree is calculated according to leaf water potential. Water flow rate from the soil to root is the same as the water flow rate in the xylem:

$$J_{soil} = K_{soil}(\psi_{soil} - \psi_{root}) = K_{soil,sat}(\psi_e/\psi_{soil})^{a_{soil}}(\psi_{soil} - \psi_{root}) \quad (9)$$

where K_{soil} is soil hydraulic conductance, $K_{soil,sat}$ is soil hydraulic conductance at saturation, ψ_e is the air entry point, a_{soil} is a parameter depending on soil characteristics (Campbell 1974). K_{soil} and $K_{soil,sat}$ can be calculated from soil hydraulic conductivity, root length index, average root radius and assumption for a

radius of a cylinder of soil to which a root has access to (Duursma et al. 2008). The total soil-to-leaf hydraulic conductance (K_{tot}) is thus ${K_{tot}}^{-1} = {K_x}^{-1} + {K_{\mathrm{soil}}}^{-1}$.

Leaf-area specific phloem transport rate (J_p) is as follows:

$$J_p = K_p C_{leaf} (P_{leaf} - P_{\mathrm{sin}\,k})/\eta(C_{leaf}) \quad (10)$$

where K_p is phloem hydraulic conductance (which is dependent on temperature and sugar concentration due to its viscosity dependence), P_{leaf} and P_{root} are the turgor pressures in the leaf and root, and $\eta(C_{leaf})$ is viscosity (in relation to pure water).

Xylem and phloem water potential (ψ) are at equilibrium both in the leaves (source) and roots (sink).

$$\psi = P - CRT \quad (11)$$

where C and P are the sugar concentration and turgor pressure (either leaf or sink phloem), R is the molar gas constant and T is the temperature (K).

The phloem loading rate of sugars was made to equal the photosynthesis rate. For the sake of simplicity, phloem loading was treated as a passive process with infinite diffusion conductance from mesophyll to source phloem so that osmotic concentration in the loading phloem is the same as in the mesophyll cells.

Sugar utilization in sinks Sugar unloading rate, i.e., sugar utilization rate in sinks (U), is typically described as a function of phloem sugar concentration at the sink with a Michaelis–Menten type function (Thompson and Holbrook 2003). However, if phloem unloading is not made water potential-dependent also, then the turgor pressure at the sink could turn negative when soil water potential and/or soil hydraulic conductance decreases substantially. We therefore subtracted a water potential term from the sugar concentration when describing the unloading rate.

$$U = \frac{\alpha_{\mathrm{sink}}(C_{\mathrm{sink}} - \psi_{\mathrm{sink}}/RT)}{(C_{\mathrm{sink}} - \psi_{\mathrm{sink}}/RT) + \beta_{\mathrm{sink}}} \quad (12)$$

where α_{sink} and β_{sink} are the parameters. In practice, this formulation means that phloem unloading is turgor dependent, as has been hypothesized to be the case (Patrick 2013). At least growth is known to be affected by turgor pressure due to its role in cell wall expansion, cell wall synthesis and protein synthesis (Fatichi et al. 2014). In any case, the difference between sugar concentration and turgor-dependent unloading will only appear in the case when soil water potential and/or soil hydraulic conductance decrease substantially, i.e., during drought. In the simulations where temperature was varied (in Figure 5A), the sink strength paratemeter α_{sink} was also made to change with ambient temperature according to a Q_{10} type equation with a Q_{10} value of 2 (Nobel 2005).

Model runs with numerical model As the whole set of coupled Eqs (1)–(12) cannot be solved analytically without some assumptions relaxed, we resort to a numerical steady-state solution of these equations where the transpiration rate (E in Eq. (2)) is set to the xylem transport rate (J_x in Eq. (8)), and the CO_2 assimilation rate (A in Eq. (1)) to phloem transport rate (J_p in Eq. (10)) and the rate of sugar utilization in the sinks (U in Eq. (12)). The equations were solved iteratively using a self-made algorithm in Fortran 90. Briefly, stomatal conductance is increased from zero upwards. For each stomatal conductance and environmental driving variables one combination of photosynthesis rate, transpiration rate, xylem water potential at source and sink, phloem pressure and concentrations at source and sink is found where the system is in steady state. The algorithm then chooses the stomatal conductance that yields the highest photosynthesis rate.

In the Results section we first demonstrate model behaviour in terms of varying leaf diffusive conductance (caused by changes in stomatal conductance) with a standard set of parameters and environmental driving variables (Table 1). We then use the model to find the leaf diffusive conductance which maximizes the simultaneous photosynthesis, phloem transport and sink sugar utilization rate as a function of environmental conditions and structural parameters, i.e., use the model to predict the optimal leaf diffusive conductance when each of the environmental conditions and structural parameters are varied. Next, we find the numerical optimal solution for leaf diffusive conductance when light level, VPD, ambient CO_2 concentration and tree structural and functional properties are varied together. We compare our solution to the analytical solution of leaf diffusive conductance given by the unified stomatal conductance model (Medlyn et al. 2011), which has been tested in field conditions at numerous sites (Lin et al. 2015), and to the analytical solution given by the optimal stomatal control model (Hari et al. 1986).

Laboratory measurements

We performed experiments on Scots pine (*Pinus sylvestris* L.) seedlings in the laboratory to verify that there is a relationship between leaf osmotic concentration and non-stomatal limitation to photosynthesis expressed in Eq. (6). The seedlings of ~1 m in height and 2 cm diameter at base were brought inside the lab approximately 1 week before the measurements and were well watered. During the experiment, they were kept in constant environmental conditions (PAR ~400 μmol m^{-2} s^{-1}, VPD ~0.01 mol mol^{-1}, ambient CO_2 concentration ~450 ppm, temperature ~22 °C) for 3–8 h. The needles inside the cuvette were kept in the same environmental conditions as the other needles. After a stabilisation period of ~1 h, some of the seedlings (n = 3) were girdled and some were notched (n = 4) on the branch, ~20 cm from the point of measurement of leaf gas exchange, while some seedlings were kept intact (n = 3). Girdling and notching treatments were used to make the water and osmotic potentials and

leaf gas exchange vary as much as possible. Notching was done by incising the xylem in one location with a razor blade in order to decrease xylem hydraulic conductance and thus leaf water potential (Sperry et al. 1993). Girdling was done to prevent phloem transport below the girdle to increase leaf sugar concentration and cause sink limitation without a decrease in leaf water potential. During the experiments, leaf gas exchange (water and CO_2) was measured with a flow-through gas exchange measurement system (GFS-3000, Walz, Effeltrich, Germany), leaf osmotic concentration was measured with a freezing point osmometer (Osmomat-030, Gonotec, Berlin, Germany) and water potential was measured with a PMS pressure chamber. Note that the osmometer actually measures osmolality (units: mol kg^{-1}), but we approximate this to be the same as osmotic concentration (units: mol l^{-1}) since these two are very close to each other in dilute solutions such as ours. Needles for the osmotic concentration and water potential measurements were collected close to the point of leaf gas exchange measurements. For the osmotic concentration measurements three to five pairs of needles were first sealed in set in silica-based membrane collection tubes (GeneJET Plasmid Miniprep Kit, Thermo Scientific, Waltham, MA, USA) and then dipped in liquid nitrogen and stored at −80 °C. Within a week, they were thawed and centrifuged at 14,000 *g* for 10 min (Heraeus Fresco 17, Thermo Scientific). The resulting sap was measured with the osmometer without delay. Measurements were conducted in May and June in 2015 in the laboratory at the Department of Forest Sciences in Helsinki University. The gross photosynthesis rate (A) was calculated by adding the respiration rate to the net CO_2 assimilation rate (assumed constant as temperature was kept constant) from the net leaf CO_2 exchange rate. Respiration rate was measured at the beginning and end of the experiment by keeping the seedling in the dark for at least 15 min. Since the light and ambient CO_2 levels were kept constant and the variation in C_i was so small in our experiments, changes in non-stomatal limitations to photosynthesis (ϕ in Eq. (6)), were calculated from the A to C_i ratio (see Figures S1 and S2 available as Supplementary Data at *Tree Physiology* Online).

Results

Leaf transpiration and CO_2 exchange rates started to decrease, and leaf osmotic concentration started to increase shortly after the notching and girdling experiments (Figure S3 available as Supplementary Data at *Tree Physiology* Online). Leaf water potential started to decrease in the notching experiment while it remained rather constant in the girdling experiment (Figure S3 available as Supplementary Data at *Tree Physiology* Online). The ratio between the gross photosynthesis rate (A) and leaf internal CO_2 concentration (C_i) (representing ϕ in Eq. (6)) was found to be well described by leaf osmotic concentration when all of the measurement points were pooled together (Figure 2A, $R^2 = 0.60$, $N = 58$, $P < 0.001$) as was assumed in our model formulation (Eq. (6)). The A/C_i ratio correlated also with leaf water potential, when all of the experiments were pooled together (Figure 2B, $R^2 = 0.32$, $N = 58$, $P < 0.001$). However, the correlation between water potential and A/C_i ratio was not as strong as the correlation between leaf osmotic concentration and A/C_i. This was due to the girdling experiments where the correlation between leaf water potential and osmotic potential was broken down (not shown) due to sink limitation, and where a strong correlation was found between A/C_i and osmotic concentration ($R^2 = 0.44$, $N = 22$, $P < 0.001$), but not between A/C_i and leaf water potential ($R^2 = 0.02$, $N = 18$, $P > 0.05$).

Figure 3 demonstrates steady-state relations in leaf (source), phloem and stem base (connected to the sink in roots) when leaf diffusive conductance changes (due to changes in stomatal conductance) using the base case parameterization shown in Table 1. Leaf internal CO_2 concentration increased with increasing stomatal conductance (Figure 3A). Simultaneously, the non-stomatal limitations to photosynthesis increased, i.e., ϕ, decreased (Figure 3A) due to an increase in leaf osmotic concentration (Figure 3B). Leaf osmotic concentration increased in line with decreasing water potential (Figure 3A) with the opening of the stomata so that turgor pressure was maintained at a value that allows the steady-state transport of the photosynthesized sugars in the phloem (Figure 3B). Leaf water potential decreased slightly faster than the transpiration rate increased due to gradual loss of xylem hydraulic conductance due to cavitation (Figure 3A). Phloem conductance decreased with increasing sugar concentration due to increased phloem sap viscosity (Figure 3B). An increasing stomatal conductance led to a decreasing water potential in the xylem, including the sink, while the maximum sink turgor pressure and osmotic concentration were found at an intermediate stomatal conductance (Figure 3C). The maximum photosynthesis rate, phloem transport rate and sink sugar utilization rates were all found at exactly the same intermediate value of stomatal conductance where the product of internal CO_2 concentration and ϕ (for photosynthesis), sugar concentration, turgor pressure gradient, and phloem conductance (for phloem transport) and sink turgor pressure (for sink sugar utilization) were at their maximum. This value of stomatal conductance where the metabolic rate was maximized was then searched iteratively in the numerical simulations that follow. No solutions to Eqs (8) and (9) were found for very large stomatal conductances (larger than shown in Figure 3) or for very low soil water potentials, due to the fact that there is an upper limit to xylem transport capacity due to run-away cavitation (Tyree and Sperry 1988, Hölttä and Nikinmaa 2013).

Figure 4 demonstrates schematically the photosynthesis rate as a function of leaf internal CO_2 concentration (C_i) when the ambient CO_2 concentration is constant. Starting from point a, stomatal opening increases C_i and movement along the A–C_i curve where $\phi = 1$ to the upper right diagonal direction. But at the same time, stomatal opening causes ϕ to decrease as sugar concentration increases to a new steady-state value between

photosynthesis and phloem transport, thus forcing a movement from the $\phi = 1$ curve to a lower A–C_i curve ($\phi = 0.8$ in this case), i.e., towards increased non-stomatal limitations, to point *b*. The key feature here is that movement along a given A–C_i curve is associated with a simultaneous movement down to a lower A–C_i curve due to increasing non-stomatal limitation. The factors that decrease A with increases in stomatal conductance due to non-stomatal limitations in photosynthesis are the ones that increase leaf sugar concentration with increases in stomatal conductance. For example, lower xylem and phloem conductances, a lower sink strength and a higher VPD will make A decrease more for a given increase in stomatal conductance. In this case, the

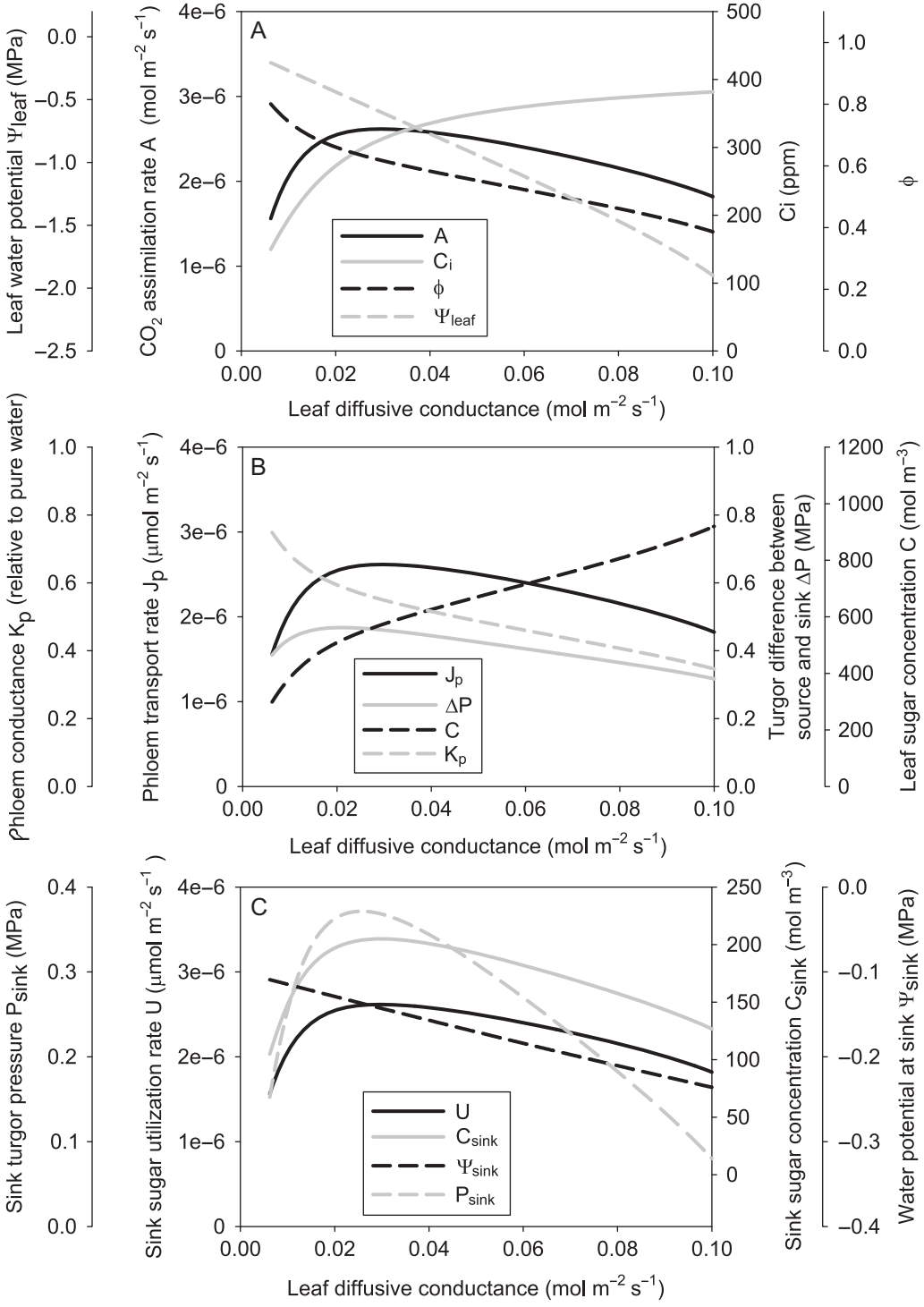

Figure 3. Model behaviour as a function of leaf diffusive conductance in terms of (A) photosynthetic production, (B) phloem transport and (C) sink sugar utilization, using base case parameterization shown in Table 1.

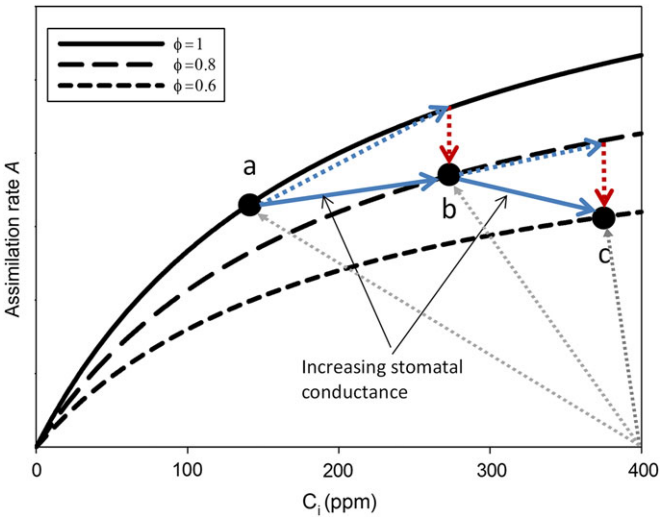

Figure 4. A schematic figure of the photosynthesis rate as a function of leaf internal CO_2 concentration C_i when ambient CO_2 concentration is held constant. Stomatal opening increases C_i and causes movement along any A–C_i curve ($\phi = 1$, $\phi = 0.8$ or $\phi = 0.6$) to the upper right diagonal direction. Stomatal opening simultaneously causes ϕ to decrease thus forcing a movement to a lower A–C_i curve. The grey dotted lines intersecting the x-axis at 400 ppm represent the supply functions of CO_2 through the stomata.

movement from a to b due to stomatal opening is desirable as point b has a higher photosynthesis rate (A) than a. A further opening of the stomata would take from point b to point c, but this would lower the photosynthesis rate and thus no further opening of the stomata is predicted to occur. The increase in photosynthesis rate for a given increase in C_i along one A–C_i curve increases with a high photosynthetic capacity (V_{cmax} and J_{max} in Eq. (5)) and high light (I in Eq. (4)), whereas the decrease to a lower A–C_i curve is more drastic with e.g. a high VPD, low xylem and phloem conductance, soil water status and sink strength, and with a low C_0, i.e., increasing sensitivity of non-stomatal limitations to photosynthesis.

The value of stomatal conductance, which maximizes the sustainable metabolic rate (i.e., the simultaneous photosynthesis, phloem transport and sink sugar utilization rate), is dependent on environmental conditions as well as on structural and functional parameters (Figure 5A). The well-known trend of increasing leaf diffusive conductance with increasing PAR (and saturation at high PAR) was captured by the model (Figure 5A). Leaf diffusive conductance was predicted to decrease with increasing VPD ($g \sim d_w^{-0.45}$, $R^2 = 0.99$) and ambient CO_2 concentration ($g \sim C_a^{-0.59}$, $R^2 = 0.96$ and $g \sim C_a^{-0.76}$, $R^2 = 0.98$ when C_a >400 ppm) (Figure 5A). Leaf diffusive conductance decreased when ambient temperature was increased in case the total amount of water in the air was kept constant, but increased slightly when the VPD was kept constant (Figure 5A). This was mainly due to increases in photosynthetic parameter V_{cmax} and J_{max} and the sink strength with increasing temperature (not shown). Leaf diffusive conductance increased with increasing xylem and phloem hydraulic conductance, and with

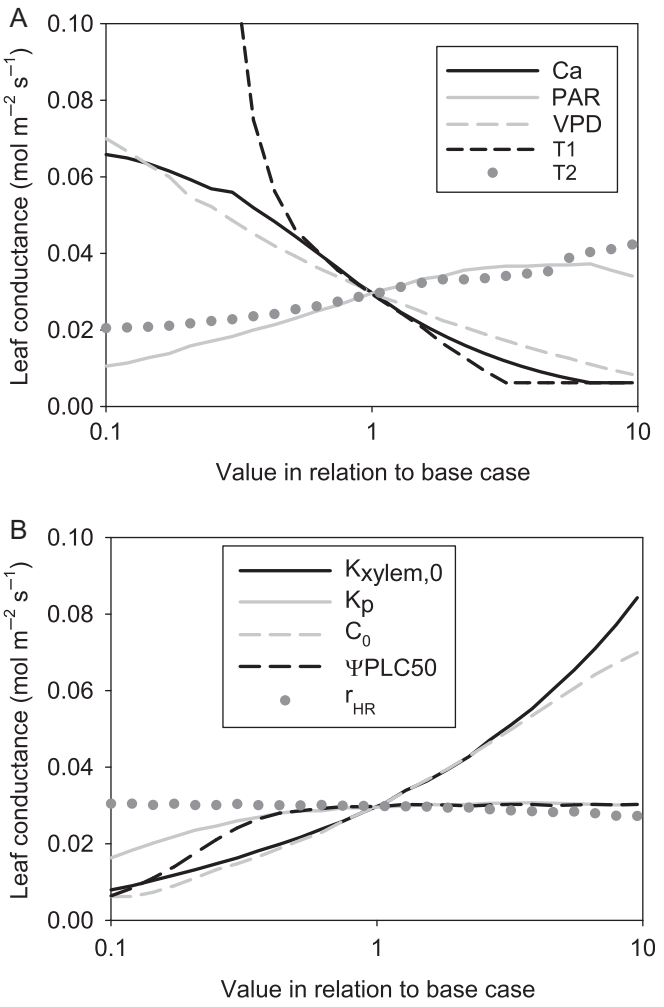

Figure 5. (A) The value of leaf diffusive conductance that maximizes the sustainable metabolic rate (i.e., the simultaneous photosynthesis, phloem transport and sink sugar utilization rate) predicted by the model as a function of VPD, light level (PAR), ambient CO_2 concentration (C_a) and ambient temperature when either absolute amount of water in the air (T_1) or VPD (T_2) was kept constant, and (B) xylem hydraulic conductance ($Kxylem,0$), phloem hydraulic conductance (K_p), leaf sugar concentration at which photosynthesis goes to zero (C_0), ψ_{PLC50} and heat transfer resistance from the leaf (rHR). Each parameter was varied independently while the others were kept at their base case values. When ψ_{PLC50} was varied, the value of the parameter a_{xylem} in Eq. (8) (the slope of the vulnerability curve) was also changed in inverse proportion to retain the proportionality between these two parameters.

decreasing ψ_{PLC50} (Figure 5B). The predicted leaf diffusive conductance was proportional to the square root of xylem hydraulic conductance ($g \sim K_x^{0.50}$, $R^2 = 0.99$), but it had an almost on-off type relation to phloem conductance and ψ_{PLC50}, with very sharp impact with low conductivity and ψ_{PLC50} values followed by almost no impact with further increase in conductivity and ψ_{PLC50}. Leaf diffusive conductance was predicted to increase with increasing C_0. Leaf diffusive conductance decreased slightly when boundary layer resistance (r_{HR}) was increased from its base case value (Figure 5B). This was due to increase in VPD associated with the increase in leaf temperature. Leaf diffusive conductance increased

along with increasing photosynthesis rate in all cases, expect with increasing C_a (see Figure S4a and b available as Supplementary Data at *Tree Physiology* Online in comparison with Figure 5). This is in line with earlier empirical stomatal conductance models (Ball et al. 1987, Medlyn et al. 2011). Non-stomatal limitations to photosynthesis generally tended to increase (decreasing ϕ) along with decreasing leaf diffusive conductance with the most notable exceptions being with respect to light and PLC50 (Figure S4c and d available as Supplementary Data at *Tree Physiology* Online in comparison with Figure 5). The relative changes in ϕ were smaller than changes in leaf diffusive conductance in all cases (not shown). When the non-stomatal limitations to photosynthesis were made to increase with decreasing leaf water potential (instead of increasing leaf sugar content), the results remained qualitatively similar with small exceptions at high light and very high ambient CO_2 concentration (Figure S5 available as Supplementary Data at *Tree Physiology* Online). In this case leaf diffusive conductance and the metabolic rate were constrained (although not to the same extent as in Figure 5) at low phloem conductance and low sink strength by limits of phloem transport to increasing viscosity with increasing phloem sugar concentration (not shown).

Figure 6 demonstrates predicted stomatal behaviour during a decreasing soil water potential. A value of 1000 μmol m^{-2} s^{-1} for light level and 0.02 mol mol^{-1} for VPD was used in these drought simulations to mimic drought conditions. In addition, a minimum leaf diffusive conductance value was set at 0.005 mol m^{-1} s^{-2}, which is ~5% of the maximum leaf diffusive conductance, to simulate cuticular water loss. In addition, we ran the simulations for different values of ψ_{PLC50}, C_O and the soil parameter a_{soil} in Eq. (9) describing the sensitivity of soil hydraulic conductance to soil water potential. Otherwise, the parameterization was as in the base case simulations. Leaf diffusive conductance was unaffected by soil water potential at high soil water potentials until it started to decrease after a threshold water potential (Figure 6A). This threshold soil water potential was dependent on many factors, for example the value of parameter a_{soil}, ψ_{PLC50} and C_O (Figure 6A). After a given threshold in soil water potential, the plant was operating at the minimum leaf diffusive conductance. This leaf conductance was maintained only for a short range of soil water potentials after which run-away cavitation occurred (corresponding to soil water potentials for which no solution was found, Figure 6A). Stomatal closure was steeper with decreasing soil water potential when soil hydraulic conductance was more sensitive to soil water potential (high a_{soil}), a more vulnerable xylem to cavitation (high ψ_{PLC50}) and more vulnerable photosynthesis to the increase in leaf osmotic concentration (low C_O) (Figure 6A). Percentage loss of conductivity (PLC) remained rather close to zero until soil water potentials close to hydraulic failure (Figure 6B). Non-stomatal limitations to photosynthesis started typically to increase (i.e., ϕ to decrease) at lower soil water potentials in comparison with stomatal conductance (Figure 6C). With most of the parameterizations, C_i remained rather constant or decreased slightly in the early stages of drought, and then started to increase sharply at the very late stage of drought (Figure 6D). Leaf water potential decrease during the drought was predicted to be larger (more anisohydric behaviour) when soil parameters a_{soil} and ψ_{PLC50} were low and C_O were high (Figure 6E). Leaf sugar concentration was generally predicted to increase with increasing drought intensity (Figure 6F), but its increase was relatively smaller in comparison with the decrease in leaf water potential, leading to a decrease in turgor pressure during drought (Figure 6G) as less turgor pressure was required in the leaves to transport the assimilated sugars in the phloem. Plant metabolic rate decreased with the progression of drought (Figure 6H).

Model behaviour was more complex when source strength parameters (V_{cmax} and J_{max} in Eqs (4) and (5)) and sink strength parameter α_{sink} in Eq. (12) were varied simultaneously (Figure 7). An increasing sink (Figure 7A) or source (Figure 7B) strength increased the leaf diffusive conductance up to a certain point, after which it plateaued. The increase in leaf diffusive conductance with increasing sink or source strength was more pronounced when accompanied by a high source or sink strength, respectively. The maximum sustainable metabolic rate (photosynthesis rate, phloem transport rate and sink unloading rate) increased more with increasing sink strength when source rate was higher (Figure 7C) and increasing source strength when sink strength was higher (Figure 7D). A lower sink strength was always accompanied by a higher leaf sugar concentration (Figure 7E) as higher sugar concentrations in the sink were required for a given sink sugar utilization rate, and this was transmitted as an increased sugar concentration to the source. The effect of source strength on sugar concentration was the opposite; low source strength decreased the sugar concentration as the phloem transport need decreased (Figure 7F).

Next we compared our solution for the leaf diffusive conductance that maximized steady-state photosynthesis rate to the solution given by the unified stomatal control (Medlyn et al. 2011), i.e.,

$$g = g_0 + g_1 \frac{A}{\sqrt{d_w}\, C_a}$$

where g_0 and g_1 are parameters. Ambient CO_2 concentration (C_a), light intensity (I) and VPD (d_w) were given as input to the model, and their values were varied three-fold (both ways) around their base case values simultaneously in the sensitivity analysis. Further, we varied soil-to-leaf hydraulic conductance K_{tot} (K_x and K_{soil} in same proportion) in our simulations to see how the slope of the leaf diffusive conductance (g_1) would change. Since the unified stomatal control model uses photosynthesis rate as a predictor for stomatal conductance, a single solution for the optimal stomatal conductance cannot be obtained solely from environmental, structural and physiological parameters. Therefore, we used the assimilation rate predicted by our model as an input A to the

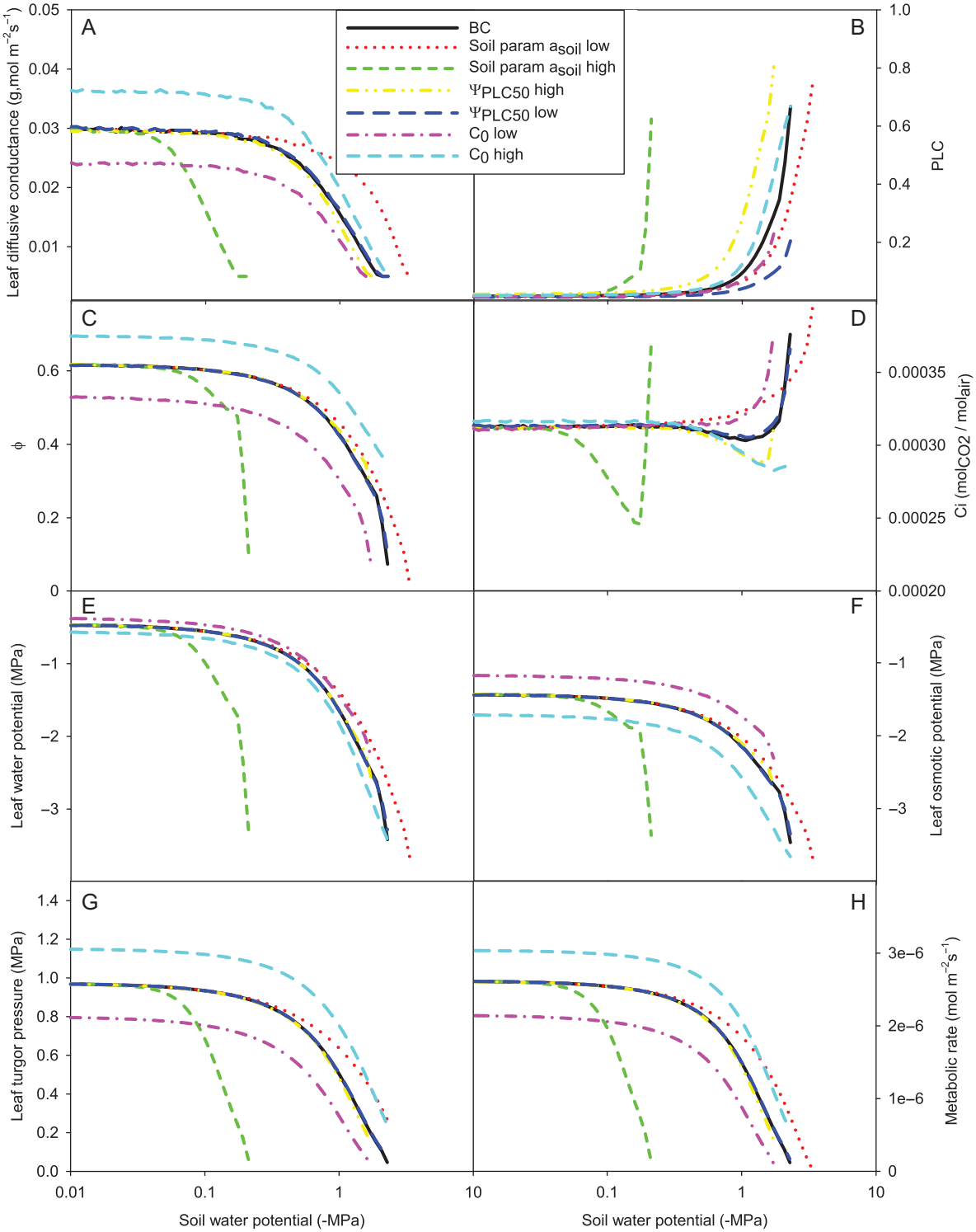

Figure 6. Model behaviour when soil water potential is decreased: (A) leaf diffusive conductance, (B) loss of xylem hydraulic conductance due to cavitation (PLC), (C) ϕ, (D) leaf internal CO_2 concentration, (E) leaf water potential, (F) leaf osmotic pressure, (G) leaf turgor pressure and (H) metabolic rate. 'BC' is for the base case simulation, 'soil param a_{soil} low' means parameterization with a_{soil} = 0.66 × base case value (soil hydraulic conductance is less sensitive to soil water potential), 'soil param a_{soil} high' means parameterization with a_{soil} = 1.2 × base case value (soil hydraulic conductance is more sensitive to soil water potential), 'ψ_{PLC50} low' means parameterization ψ_{PLC50} = 0.5 × base case value, 'ψ_{PLC50} high' means parameterization ψ_{PLC50} = 2 × base case value, 'C_0 low' means parameterization with C_0 = 0.5 × base case value, 'C_0 high' means parameterization with C_0 = 2 × base case value.

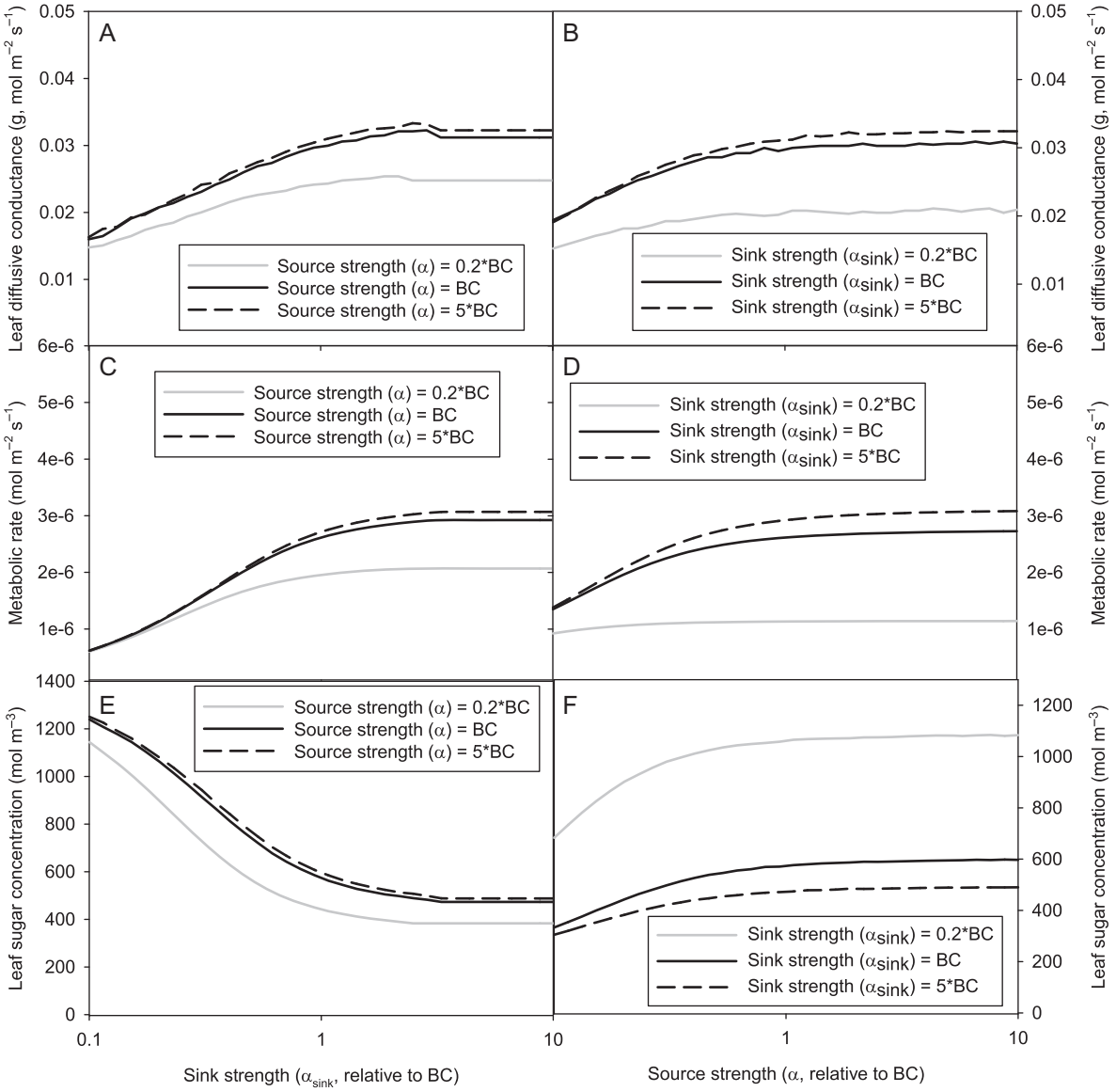

Figure 7. Model behaviour when source strength (V_{cmax} and J_{max} in Eqs (4) and (5)) and sink strength (α_{sink} in Eq. (12)) are varied simultaneously: (A and B) leaf diffusive conductance maximizing metabolic rate, (C and D) the maximum sustainable metabolic rate, and (E and F) leaf osmotic potential. 'BC' refers to base case parameterization given in Table 1.

unified stomatal control model. In doing the model comparison, we used only the light-limited side of photosynthesis function (i.e., Eq. (4)) so that our analysis would agree with the assumptions in Medlyn et al. (2011). Our model predictions agreed quite well with the prediction of the unified stomatal control model, i.e., the prediction that there should be a linear relationship between g and $A/(\mathrm{sqrt}(d_w) \times C_a)$ (Figure 8A, black points $R^2 = 0.93$). When we further varied K_{tot} our results continued to agree with predictions by unified stomatal control model while the slope g_1 changed (Figure 8). The slope g_1 increased approximately in proportion to the square root of soil-to-leaf hydraulic conductance ($g_1 \sim K_{tot}^{0.40}$, Figure 8B). Also changes in other structural and functional properties affected the slope (such as α_{sink}, C_O), but to a much lesser extent, and not so clearly as the soil-to-leaf hydraulic conductance (not shown) as their effect on the predicted stomatal conductance was mediated mainly through changes in A, whereas changes in K_{tot} affected both A and the slope g_1.

Finally, we compared our numerical solution to the solution given by the optimal stomatal control model (Hari et al. 1986):

$$g = \left(\sqrt{\frac{C_a}{\lambda d_w}} - 1\right) f = \left(\sqrt{\frac{C_a}{\lambda d_w}} - 1\right) \frac{\alpha I}{I + \beta}$$

where λ is the 'marginal cost of water' (which was fitted to get a good fit between g and the environmental drivers d_w and I), and α and β are the light response parameters of photosynthesis (Hari et al. 1986), which were given values of 0.08 mol m^{-2} $s^{-1}$and 1000 μmol m^{-2} s^{-1}, respectively. These values for α and β were

chosen so that the photosynthetic light-response would be similar to the Farquhar model parameterization in our model. Now VPD (d_w) and light (I) were varied three-fold (both ways) around their base case values simultaneously, while C_a was kept constant as the optimal stomatal model gives contradictory C_a responses (assuming constant λ). Again, the predictions of the two models were similar (Figure 9A black points, $R^2 = 0.99$), although there was more non-linearity in comparison with the unified stomatal control model. This may be at least partly due to the fact the optimal stomatal conductance model uses a different form of the photosynthesis function (Hari et al. 1986). When K_{tot} was varied and λ was fitted to the data, λ was found to increase approximately in proportion to $1/K_{tot}$ ($\lambda \sim K_{tot}^{-0.84}$, Figure 9B) and the fit between the optimal stomatal model and our model remained reasonable (Figure 9A all points, $R^2 = 0.97$). Also changes in other structural and functional parameters affected λ, e.g., it decreased with increasing sink strength (α_{sink}) and C_O (Figure S6 available as Supplementary Data at *Tree Physiology* Online). Our results imply that the marginal water cost of carbon gain (λ) in the optimal stomatal conductance model is approximately inversely proportional to soil-to-leaf hydraulic conductance and g_1 in the unified stomatal control model is proportional to the square root of soil-to-leaf hydraulic conductance, i.e., leaf diffusive conductance is proportional to the square soil-to-leaf hydraulic conductance. This is in line with the interpretation that g_1 is proportional to the square root of the marginal water cost of carbon gain (λ) (Medlyn et al. 2011). Note that the definition of λ in equation above after Hari et al. (1986) and Mäkelä et al. (1996) is the inverse of the definition of λ in the formulation by Cowan and Farquhar (1977) and Medlyn et al. (2011). In both model comparisons, changes in VPD (d_w) and soil-to-leaf hydraulic conductance (K_{tot}) affect the predicted stomatal conductance exactly in

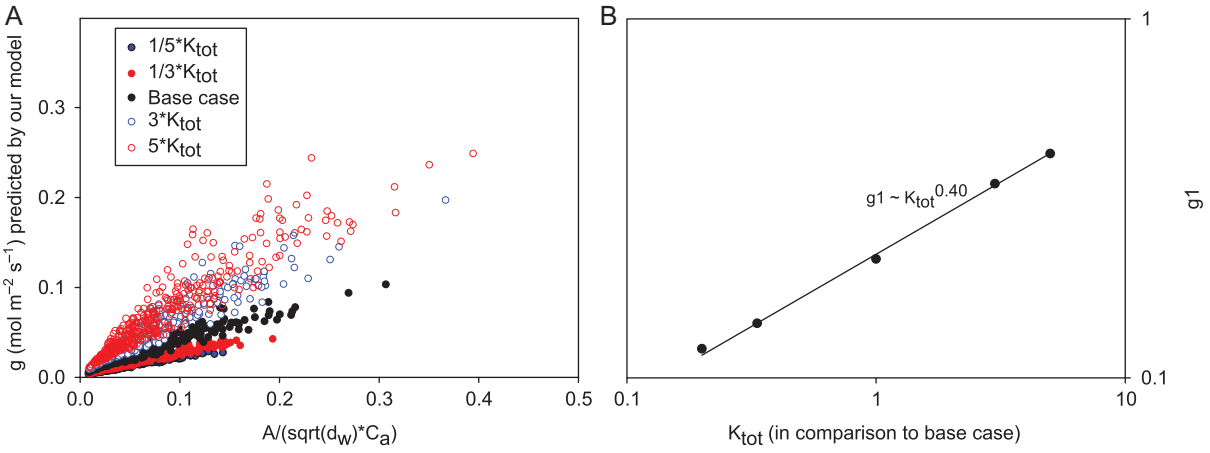

Figure 8. (A) Comparison of our model behaviour with the unified stomatal control model (e.g. Medlyn et al. 2011) when PAR (I), Ca and VPD (d_w) are varied simultaneously using different values for soil-to-leaf hydraulic conductance (K_{tot}). The values for all of the other parameters were kept as in the previous simulations, i.e., the base case values shown in Table 1. (B) Value of g1 fitted as a function of soil-to-leaf hydraulic conductance (K_{tot}).

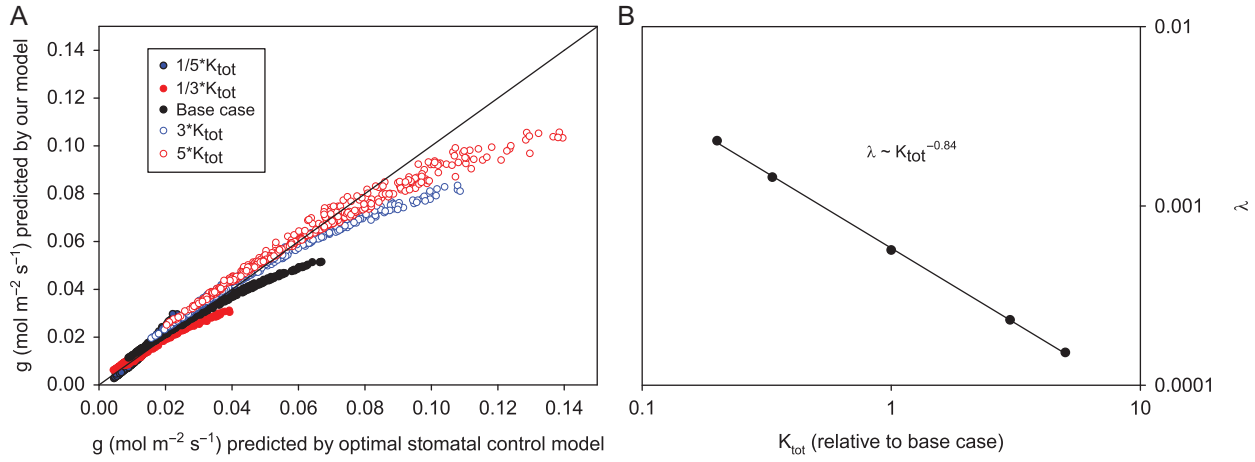

Figure 9. (A) Comparison of our model behaviour with the optimal stomatal control model (Hari et al. 1986) when PAR (I) and VPD (d_w) are varied simultaneously using different values for soil-to-leaf hydraulic conductance (K_{tot}). The values for all of the other parameters were kept as in the previous simulations, i.e., the base case values shown in Table 1. (B) Value of λ fitted as a function of soil-to-leaf hydraulic conductance (K_{tot}).

the opposite manner (not shown), as their effect on leaf water potential is the opposite, i.e., $\psi_{leaf} \sim K_{tot}/d_w$.

Discussion

Carbon-assimilating leaves and carbon sinks are connected to each other through xylem and phloem so a key task of stomatal regulation is to match leaf gas exchange to the internal circulation of sap in trees. When water potential or sugar concentration of one tissue within a tree changes, xylem and phloem propagate this change to other tissues (Pantin et al. 2012, Nikinmaa et al. 2013). Since the rate of both source and sink processes are dependent on local water and carbohydrate status, any change in sink status will be reflected to source status and vice versa. Our numerical analysis utilizing this theoretical framework demonstrates that the previously well-known responses of stomatal behaviour are in good agreement with maximizing the photosynthesis rate in steady state when the above source–sink connection and tree hydraulics are considered (Figures 5 and 6). The results from our numerical solution are very similar to the results from the widely applicable unified stomatal conductance model (Medlyn et al. 2011, Lin et al. 2015) (Figure 7), and thus also very similar to the solutions by Ball et al. (1987) and Leuning (1995). In addition, our model makes stomatal behaviour directly responsive to drought conditions and cases of sink limitation. Our model provides a potential explanation for the marginal water cost in the unified stomatal conductance model and optimal stomatal model, which until now have been estimated through empirical parameter fitting and been found to vary between plant functional types and in different environments (Kolari et al. 2007, Prentice et al. 2014, Lin et al. 2015), or been described as a function of soil water content to maximize carbon gain under the constraint of finite soil water availability (Mäkelä et al. 1996, Manzoni et al. 2013).

In our steady-state model simulations the stomatal and non-stomatal limitations to photosynthesis are tightly coupled (Figure 8). In essence, our prediction is similar also in this aspect to the prediction by the models of Ball et al. (1987), Leuning (1995), Medlyn et al. (2011) and Hari and Mäkelä (2003) since in these models leaf diffusive conductance is proportional to photosynthesis rate. The wide usability of these models would suggest that such linking is frequent in trees. In our approach, the linking arises since assuming the feedback between the rate of photosynthesis and photosynthate accumulation allows us to find a leaf diffusive conductance that balances gas exchange with sap circulation at a maximum possible photosynthetic rate. It has been evident for a long time that, at least at the longer time scale, e.g., during the progression of a drought, stomatal and non-stomatal limitations to photosynthesis are coordinated with each other (Flexas and Medrano 2002, Manzoni 2014, Zhou et al. 2014). In addition, recent reviews have highlighted the dynamic nature of mesophyll conductance; mesophyll conductance can change as fast as stomatal conductance, i.e., within seconds or minutes (Flexas et al. 2008, 2012, Kaiser et al. 2015) and regardless of how fast the environmental conditions change (Flexas et al. 2012). Typically mesophyll conductance has been found to change in parallel with stomatal conductance (Flexas et al. 2008), and midday depression of photosynthesis has been attributed to both stomatal and non-stomatal limitations to photosynthesis, even during non-drought conditions (Zhang and Gao 2000, Mediavilla et al. 2002, Nascimento and Marenco 2013). The reasons for changes in mesophyll conductance are not well understood, but factors that may contribute to variations in it are, e.g., changes in carbonic anhydrase, aquaporin activity and the area of chloroplasts facing intercellular spaces (Kaiser et al. 2015). We further hypothesize that one additional purely physical candidate for affecting mesophyll conductance could be the decrease in the aqueous phase diffusion coefficient for CO_2 with increasing sugar concentration (Carroll et al. 2014).

Most of the studies have linked increases in non-stomatal limitations to photosynthesis to water stress, but also increasing sugar and starch concentration in leaves have been found to decrease photosynthetic production (Nafziger and Koller 1976, Goldschmidt and Huber 1992, Myers et al. 1999, Iglesias et al. 2002). More specifically, increasing leaf sugar concentrations have been found to increase non-stomatal limitations to photosynthesis (Turnbull et al. 2002, Franck et al. 2006, Hüve et al. 2006, Quentin et al. 2013, Kitao et al. 2015). However, the functional form of the relation between the decrease in A for a given C_i and light with increasing leaf sugar concentration has not been quantitatively and extensively tested (but see, e.g., Franck et al. 2006 and our experimental results in Figure 2). In general, it might be difficult to distinguish between the effects of leaf water potential vs sugar concentration on photosynthesis since these two are so intimately linked to each other unless sink strength is changing or active osmoregulation is occurring.

Our modelling results also demonstrate (Figure 6A vs C) that the changes in non-stomatal limitations need not be extremely large to influence leaf diffusive conductance since the concurrent decrease in leaf diffusive conductance will prevent the non-stomatal limitations from decreasing excessively. Our analysis thus highlights the need for more studies on the nature of the non-stomatal limitations to photosynthesis and how they respond to changes in leaf water and sugar status. In any case, our results show that formulating such a feedback allows linking stomatal conductance with whole-tree-level water and source–sink relationships and provides very realistic stomatal behaviour. If this feedback is excluded from the model, then the maximum steady-state photosynthesis rate would only be limited by transport capacity of the xylem and phloem (Hölttä and Nikinmaa 2013) and feasible outcome would include unrealistically high leaf sugar concentrations with a tendency for irregular stomatal behaviour, unless other concepts such as the cost of water are introduced in the model formulation.

A range of behaviour between isohydric and anisohydric behaviour was predicted to be possible during drought, depending on the choice of the functional and structural parameters (Figure 6E). Our analysis predicts that photosynthesis is simultaneously source- and sink-limited (Figure 7). Note that by sink limitation, we mean here that the rate of sugar utilization for a given sugar concentration or turgor pressure is low, i.e., we do not distinguish whether the sugars are utilized in growth, respiration, storage, soil exudation or some other process. When source strength is very high then sink strength will start to affect photosynthetic production and vice versa. In the model results increasing source strength above a given threshold does not increase photosynthesis rate without a simultaneous increase in sink strength and vice versa (Figure 7). High source strength and low sink strength are predicted to increase osmotic concentration and turgor pressure at the sink. In the case that photosynthesis is source-limited while sink strength is very high, sugar concentration is predicted to change hand in hand with water potential, but in the case of sink limitation, leaf sugar concentration is predicted to increase much faster than leaf water potential decreases (i.e., turgor pressure increases). If sink strength decreases, then the osmotic concentration and turgor pressure at the sink have to increase even more than sink water potential decreases to maintain a constant rate of sink sugar consumption. This is reflected to the source through the phloem as an increase in both osmotic concentration and turgor pressure. Turgor pressure and osmotic concentration have to be raised even more in source in comparison with the sink in case phloem transport capacity is decreased. A high turgor pressure in the leaf is thus predicted to reflect sink limitation and a low turgor pressure source limitation (Patrick 2013). If the high leaf turgor pressure is accompanied by high sink turgor pressure, then the sink limitation is caused by insufficient sink strength. If not, then the sink limitation is caused by low phloem transport capacity.

The major limitations of our model are that (i) it is a steady-state model in which (ii) sucrose is assumed to be the only osmotic component. The steady-state assumption does not allow for buffering of short time scale imbalances between photosynthetic production rate, phloem transport rate and sink sugar utilization rate by, e.g., starch dynamics or elastic changes in tissue volume; this would require the use of a dynamic model. A dynamic analysis is very challenging since each of the processes involved in the theoretical framework can reach a steady state at different time scales ranging from less than seconds for the light reactions of photosynthesis (Porcar-Castell et al. 2014) to hours or days for the phloem sugar concentration (Thompson and Holbrook 2003). The leaf diffusive conductance that maximizes a metabolic rate would thus depend on the time scale on which that optimization problem is done on (Nikinmaa et al. 2013). However, it is possible that stomatal responses could anticipate future equilibrium states (Pantin et al. 2012, Nikinmaa et al. 2013). In fact, stomatal closure and increases in non-stomatal limitations to photosynthesis in response to a decrease in sink strength have been found to occur before noticeable accumulation of sugar and starch in the leaves (Nebauer et al. 2011). Trees are hierarchical structures and most likely leaves are in steady-state to proximal woody axes that changes dynamically as the more distal parts react to soil moisture changes. The big difference between the pressure propagation due to hydrostatic vs osmotic reasons causes an interesting further aspect to whole-tree-level response dynamics. While the transpiration-driven pressure changes propagate through a large tree in minutes, changes in sugar concentration may take days. Against that background, the assumption of sucrose being the only osmotically active substance links the sugar concentration dependence of both photosynthesis and sink sugar consumption to osmotic regulation too strongly. It does not take into account that smaller molecular mass sugars, such as glucose and fructose (Woodruff 2014), or other solutes, such as potassium, could produce a higher ratio of osmotic concentration to phloem sap viscosity, which would also have an impact on the tree-level response dynamics.

A major advantage of our approach is that it links source–sink reactions through xylem and phloem transport, offering a way to understand their mutual interactions within a tree. Our results suggest that there are thresholds of phloem conductivity and xylem vulnerability to cavitation that cause stomata to close (Figure 5B). Run-away cavitation has long been identified as a critical boundary condition for stomatal opening (Tyree and Sperry 1988). The predicted response of leaf diffusive conductance to ψ_{PLC50} and phloem conductivity are highly non-linear; excess resistance to cavitation or phloem transport capacity beyond a certain level brings only marginal benefit. A very vulnerable xylem causes leaf water potential to decrease quickly. Similarly, a very low phloem conductance causes sugars to build up in the leaves, increasing the non-stomatal limitation to photosynthesis. Above a threshold phloem conductance, sink activity limits phloem transport. One would thus expect the phloem conductance of trees to be linked to the maximum attainable photosynthetic rate, in the same way as the ψ_{PLC50} value is related to the minimum water potential a tree is likely to experience (Choat et al. 2012). It seems unlikely that trees would build extra phloem transport capacity due to its high nitrogen costs (Hölttä et al. 2013). In contrast to phloem conductance, increasing the xylem conductance increased the predicted leaf diffusive conductance (Figure 5B). Also, some previous studies indicate that xylem conductance increases faster than phloem conductance as trees grow in size (Hölttä et al. 2013). However, xylem conductance is coupled with xylem vulnerability to cavitation as both depend on the pit membrane characteristics (Cochard 2006), complicating the relationship between xylem conductance and optimum leaf diffusive conductance. It is therefore possible that the minimum vulnerability to cavitation may impose a maximum level of xylem conductivity (Gleason et al. 2016).

The present approach does not suggest a physiological mechanism for stomatal regulation but shows plant level implications

of leaf gas exchange that reproduce observed features when carbon uptake is maximized. The key dynamic feature that reflects the processes in the different parts of plant is the sugar concentration in leaves. Recently, it has been suggested that sucrose mediated by hexokinases and ABA could directly induce closing of guard cells (Kelly et al. 2013). This, together with the feedbacks from sugar sensing pathways to photosynthetic rate (Granot et al. 2013), could represent the mechanisms that generate the predicted behaviour. In any case, our approach shows a framework of physiologically quantifiable processes that produce in concert the known features of stomatal behaviour.

Supplementary Data

Supplementary Data are available at *Tree Physiology* Online.

Funding

Funding from Academy of Finland projects #268342 and #272041.

Conflict of interest

None declared.

References

Ball JT, Woodrow IE, Berry JA (1987) A model predicting stomatal conductance and its contribution to the control of photosynthesis under different environmental conditions. In: Biggins I (ed) Progress in photosynthesis research. Vol. IV, Springer, Netherlands, pp 221–224.

Barbour MM, Fischer RA, Sayre KD, Farquhar GD (2000) Oxygen isotope ratio of leaf and grain material correlates with stomatal conductance and grain yield in irrigated wheat. Funct Plant Biol 27:625–637.

Buckley TN, Diaz-Espejo A (2015) Partitioning changes in photosynthetic rate into contributions from different variables. Plant Cell Environ 38:1200–1211.

Campbell GS (1974) A simple method for determining unsaturated conductivity from moisture retention data. Soil Science 117:311–314.

Carroll NJ, Jensen KH, Parsa S, Holbrook NM, Weitz DA (2014) Measurement of flow velocity and inference of liquid viscosity in a microfluidic channel by fluorescence photobleaching. Langmuir 30:4868–4874.

Choat B, Jansen S, Brodribb TJ et al. (2012) Global convergence in the vulnerability of forests to drought. Nature 491:752–755.

Cochard H (2006) Cavitation in trees. CR Physique 7:1018–1126.

Cowan IR, Farquhar GD (1977) Stomatal function in relation to leaf metabolism and environment. In: Jennings DH (ed) Integration of activity in the higher plant. Cambridge University Press, Cambridge, pp 471–505.

De Schepper V, Steppe K (2010) Development and verification of a water and sugar transport model using measured stem diameter variations. J Exp Bot 61:2083–2099.

Duursma RA, Kolari P, Perämäki M et al. (2008) Predicting the decline in daily maximum transpiration rate of two pine stands during drought based on constant minimum leaf water potential and plant hydraulic conductance. Tree Physiol 28:265–276.

Farquhar GD, Von Caemmerer S, Berry JA (1980) A biochemical model of photosynthetic CO_2 assimilation in leaves of C3 species. Planta 149:78–90.

Fatichi S, Leuzinger S, Koerner C (2014) Moving beyond photosynthesis: from carbon source to sink-driven vegetation modeling. New Phytol 201:1086–1095.

Flexas J, Medrano H (2002) Drought-inhibition of photosynthesis in C3 plants: stomatal and non-stomatal limitations revisited. Ann Bot 89: 183–189.

Flexas J, Ribas-Carbo M, Diaz-Espejo A, Galm ES, Medrano H (2008) Mesophyll conductance to CO_2: current knowledge and future prospects. Plant Cell Environ 31:602–621.

Flexas J, Barbour MM, Brendel O et al. (2012) Mesophyll diffusion conductance to CO_2: an unappreciated central player in photosynthesis. Plant Sci 193:70–84.

Franck N, Vaast P, Génard M, Dauzat J (2006) Soluble sugars mediate sink feedback down-regulation of leaf photosynthesis in field-grown Coffea arabica. Tree Physiol 26:517–525.

Gago J, de Menezes Daloso D, Figueroa CM, Flexas J, Fernie AR, Nikoloski Z (2016) Relationships of leaf net photosynthesis, stomatal conductance, and mesophyll conductance to primary metabolism: a multispecies meta-analysis approach. Plant Physiol 171:265–279.

Gleason SM, Westoby M, Jansen S et al. (2016) Weak tradeoff between xylem safety and xylem-specific hydraulic efficiency across the world's woody plant species. New Phytol 209:123–136.

Goldschmidt EE, Huber SC (1992) Regulation of photosynthesis by end-product accumulation in leaves of plants storing starch, sucrose, and hexose sugars. Plant Physiol 99:1443–1448.

Granot D, David-Schwartz R, Kelly G (2013) Hexose kinases and their role in sugar-sensing and plant development. Front Plant Sci 4:44.

Guo WD, Guo YP, Liu JR, Mattson N (2009) Midday depression of photosynthesis is related with carboxylation efficiency decrease and D1 degradation in bayberry (*Myrica rubra*) plants. Sci Hort 123: 188–196.

Hari P, Mäkelä A (2003) Annual pattern of photosynthesis in Scots pine in the boreal zone. Tree Physiol 23:145–155.

Hari P, Mäkelä A, Korpilahti E, Holmberg M (1986) Optimal control of gas exchange. Tree Physiol 2:169–175.

Hüve K, Bichele I, Tobias M, Niinemets Ü (2006) Heat sensitivity of photosynthetic electron transport varies during the day due to changes in sugars and osmotic potential. Plant Cell Environ 29:212–228.

Hölttä T, Nikinmaa E (2013). Modelling the effect of xylem and phloem transport on leaf gas exchange. In: IX International Workshop on Sap Flow 991, 28 May 2013, pp 351–358.

Hölttä T, Mäkinen H, Nöjd P, Mäkelä A, Nikinmaa E (2010) A physiological model of softwood cambial growth. Tree Physiol 30: 1235–1252.

Hölttä T, Kurppa M, Nikinmaa E (2013) Scaling of xylem and phloem transport capacity and resource usage with tree size. Front Plant Sci 4:496.

Iglesias DJ, Lliso I, Tadeo FR, Talon M (2002) Regulation of photosynthesis through source: sink imbalance in citrus is mediated by carbohydrate content in leaves. Physiol Plant 116:563–572.

Jones HG (1992) Plants and microclimate. Cambridge University Press, Cambridge, 428 p.

Kaiser E, Morales A, Harbinson J, Kromdijk J, Heuvelink E, Marcelis LF (2015) Dynamic photosynthesis in different environmental conditions. J Exp Bot 66:2415–2426.

Kellomäki S, Wang KY (1996) Photosynthetic responses to needle water potentials in Scots pine after a four-year exposure to elevated CO2 and temperature. Tree Physiol 16:765–772.

Kelly G, Moshelion M, David-Schwartz R, Halperin O, Wallach R, Attia Z, Belausov E, Granot D (2013) Hexokinase mediates stomatal closure. Plant J 75:977–988.

Kitao M, Yazaki K, Kitaoka S et al. (2015) Mesophyll conductance in leaves of Japanese white birch (*Betula platyphylla* var. *japonica*) seedlings grown under elevated CO_2 concentration and low N availability. Physiol Plant 155:435–445.

Kolari P, Chan T, Porcar-Castell A, Bäck J, Nikinmaa E, Juurola E (2014) Field and controlled environment measurements show strong seasonal acclimation in photosynthesis and respiration potential in boreal Scots pine. Front Plant Sci 5:717.

Kolari P, Lappalainen HK, Hänninen H, Hari P (2007) Relationship between temperature and the seasonal course of photosynthesis in Scots pine at northern timberline and in southern boreal zone. Tellus 59B:542–552.

Körner C (2003) Carbon limitation in trees. J Ecol 91:4–17.

Leuning R (1995) A critical appraisal of a combined stomatal-photosynthesis model for C3 plants. Plant Cell Environ 18:339–355.

Lin YS, Medlyn BE, Duursma RA et al. (2015) Optimal stomatal behaviour around the world. Nat Clim Change 5:459–464.

Mäkelä A, Berninger F, Hari P (1996) Optimal control of gas exchange during drought: theoretical analyses. Ann Bot 77:461–467.

Manzoni S (2014) Integrating plant hydraulics and gas exchange along the drought-response trait spectrum. Tree Physiol 34:1031–1034.

Manzoni S, Vico G, Palmroth S, Porporato A, Katul G (2013) Optimization of stomatal conductance for maximum carbon gain under dynamic soil moisture. Adv Water Resour 62:90–105.

McDowell NG, Beerling DJ, Breshears DD, Fisher RA, Raffa KF, Stitt M (2011) The interdependence of mechanisms underlying climate-driven vegetation mortality. Trends Ecol Evol 2:523–532.

Mediavilla S, Santiago H, Escudero A (2002) Stomatal and mesophyll limitations to photosynthesis in one evergreen and one deciduous Mediterranean oak species. Photosynthetica 40:553–559.

Medlyn BE, Duursma RA, Eamus D et al. (2011) Reconciling the optimal and empirical approaches to modelling stomatal conductance. Glob Chang Biol 17:2134–2144.

Meir P, Kruijt B, Broadmeadow M, Kull O, Carswell F, Nobre A, Jarvis PG (2002) Acclimation of photosynthetic capacity to irradiance in tree canopies in relation to leaf nitrogen concentration and leaf mass per unit area. Plant Cell Environ 25:343–357.

Mencuccini M, Minunno F, Salmon Y, Martínez-Vilalta J, Hölttä T (2015) Coordination of physiological traits involved in drought-induced mortality of woody plants. New Phytol 208:396–409.

Myers DA, Thomas RB, DeLucia EH (1999) Photosynthetic responses of loblolly pine (*Pinus taeda*) needles to experimental reduction in sink demand. Tree Physiol 19:235–242.

Nafziger ED, Koller HR (1976) Influence of leaf starch concentration on CO_2 assimilation in soybean. Plant Physiol 57:560–563.

Nascimento HC, Marenco RA (2013) Mesophyll conductance variations in response to diurnal environmental factors in *Myrcia paivae* and *Minquartia guianensis* in Central Amazonia. Photosynthetica 51: 457–464.

Nebauer SG, Renau-Morata B, Guardiola JL, Molina RV (2011) Photosynthesis down-regulation precedes carbohydrate accumulation under sink limitation in *Citrus*. Tree Physiol 31:169–177.

Nikinmaa E, Hölttä T, Hari P, Kolari P, Mäkelä A, Sevanto S, Vesala T (2013) Assimilate transport in phloem sets conditions for leaf gas exchange. Plant Cell Environ 36:655–669.

Nobel PS (2005) Physicochemical and environmental plant physiology. Academic Press, San Diego, CA.

Pantin F, Simonneau T, Muller B (2012) Coming of leaf age: control of growth by hydraulics and metabolics during leaf ontogeny. New Phytol 196:349–366.

Pammenter NW, Van der Willigen C (1998) A mathematical and statistical analysis of the curves illustrating vulnerability of xylem to cavitation. Tree Physiol 18:589–593.

Patrick JW (2013) Does Don Fisher's high-pressure manifold model account for phloem transport and resource partitioning? Front Plant Sci 4:184.

Paul MJ, Foyer CH (2001) Sink regulation of photosynthesis. J Exp Bot 52:1383–1400.

Paul MJ, Pellny TK (2003) Carbon metabolite feedback regulation of leaf photosynthesis and development. J Exp Bot 5:539–547.

Pfautsch S, Renard J, Tjoelker MG, Salih A (2015) Phloem as capacitor: radial transfer of water into xylem of tree stems occurs via symplastic transport in ray parenchyma. Plant Physiol 167: 963–971.

Prentice IC, Dong N, Gleason SM, Maire V, Wright IJ (2014) Balancing the costs of carbon gain and water transport: testing a new theoretical framework for plant functional ecology. Ecol Lett 17:82–91.

Porcar-Castell A, Tyystjärvi E, Atherton J et al. (2014) Linking chlorophyll a fluorescence to photosynthesis for remote sensing applications: mechanisms and challenges. J Exp Bot 65:4065–4095.

Quentin AG, Close DC, Hennen LMHP, Pinkard EA (2013) Down-regulation of photosynthesis following girdling, but contrasting effects on fruit set and retention, in two sweet cherry cultivars. Plant Physiol Biochem 73:359–367.

Rodriguez-Dominguez CM, Buckley TN, Egea G, Cires A, Hernandez-Santana V, Martorell S, Diaz-Espejo A (2016) Most stomatal closure in woody species under moderate drought can be explained by stomatal responses to leaf turgor. Plant Cell Environ 39:2014–2026.

Sevanto S, McDowell NG, Dickman LT, Pangle R, Pockman WT (2014) How do trees die? A test of the hydraulic failure and carbon starvation hypotheses. Plant Cell Environ 37:153–161.

Sharkey TD, Bernacchi CJ, Farquhar GD, Singsaas EL (2007) Fitting photosynthetic carbon dioxide response curves for C3 leaves. Plant Cell Environ 3:1035–1040.

Sperry JS, Alder NN, Eastlack SE (1993) The effect of reduced hydraulic conductance on stomatal conductance and xylem cavitation. J Exp Bot 44:1075–1082.

Steppe K, Sterck F, Deslauriers A (2015) Diel growth dynamics in tree stems: linking anatomy and ecophysiology. Trends Plant Sci 20:335–343.

Thompson MV, Holbrook NM (2003) Application of a single-solute non-steady-state phloem model to the study of long-distance assimilate transport. J Theor Biol 220:419–455.

Thum T, Aalto T, Laurila T, Aurela M, Kolari P, Hari P (2007) Parametrization of two photosynthesis models at the canopy scale in a northern boreal Scots pine forest. Tellus B 59:874–890.

Turgeon R (2010) The role of phloem loading reconsidered. Plant Physiol 152:1817–1823.

Turnbull MH, Murthy R, Griffin KL (2002) The relative impacts of daytime and night-time warming on photosynthetic capacity in *Populus deltoides*. Plant Cell Environ 25:1729–1737.

Tuzet A, Perrier A, Leuning R (2003) A coupled model of stomatal conductance, photosynthesis and transpiration. Plant Cell Environ 26: 1097–1116.

Tyree MT, Sperry JS (1988) Do woody plants operate near the point of catastrophic xylem dysfunction caused by dynamic water stress? Answers from a model. Plant Physiol 88:574–580.

Woodruff DR (2014) The impacts of water stress on phloem transport in Douglas-fir trees. Tree Physiol 34:5–14.

Wullschleger SD (1993) Biochemical limitations to carbon assimilation in C3 plants—a retrospective analysis of the A/Ci curves from 109 species. J Exp Bot 44:907–920.

Zhang S, Gao R (2000) Diurnal changes of gas exchange, chlorophyll fluorescence, and stomatal aperture of hybrid poplar clones subjected to midday light stress. Photosynthetica 37:559–571.

Zhou S, Duursma RA, Medlyn BE, Kelly JWG, Prentice IC (2013) How should we model plant responses to drought? An analysis of stomatal and non-stomatal responses to water stress. Agric For Meteorol 182: 204–214.

Zhou S, Medlyn B, Sabaté S, Sperlich D, Prentice IC (2014) Short-term water stress impacts on stomatal, mesophyll, and biochemical limitations to photosynthesis differ consistently among tree species from contrasting climates. Tree Physiol 34:1035–1046.